Clumping in Hot Star Winds
W.-R. Hamann, A. Feldmeier & L.M. Oskinova, eds.
Potsdam: Univ.-Verl., 2008
URN: http://nbn-resolving.de/urn:nbn:de:kobv:517-opus-13981

Rapidly accelerating clumps in the winds of the very hot WNE Stars

A.-N. Chené[1], A.F.J. Moffat[1] & P.A. Crowther[2]
[1] *Université de Montréal, Canada*
[2] *University of Sheffield, UK*

We study the time variability of emission lines in three WNE stars : WR 2 (WN2), WR 3 (WN3ha) and WR152 (WN3). While WR 2 shows no variability above the noise level, the other stars do show variation, which are like other WR stars in WR 152 but very fast in WR 3. From these motions, we deduce a value of $\beta \sim 1$ for WR 3 that is like that seen in O stars and $\beta \sim 2$–3 for WR 152, that is intermediate between other WR stars and WR 3.

1 Clumping in Wolf-Rayet Winds

Previously in these proceedings, one of us (AFJM) showed how the motion of subpeaks over the broad emission lines in the spectra of Wolf-Rayet (WR) stars can be associated with the motion of clumps in the wind. He also reminded us how Lépine & Moffat (1999) followed the trajectory of subpeaks in the spectra of 9 WR stars and determine their velocity law, with the assumption of a β-law for which a value of βR_* is calculated (R_* is the radius of the base of the wind). For all these stars, the value of βR_* found ranges between 20 and 80 $R_\odot$. Taking the values of stellar radius from the literature and assuming that the base of the wind is at this radius, they obtained values for β which are much greater than 1, indicating that the WR winds have very slow acceleration. However, all the stars studied by Lépine & Moffat (1999) are WC or WNL stars showing broad emission lines formed at radii where the wind has reached a velocity near terminal (v_∞) while none of them are hot, weak-line WNE stars.

2 The Spectrum of WR2, WR3 and WR152

In this study, we were initially interested in the spectrum of WR3, which shows weak, narrow triangular emission lines (Marchenko et al. 2004), indicating that, in contrast to the previously studied WR stars, the lines in WR3 come from regions of great acceleration, i.e. regions at radii near the base of the wind. If we can assume that the wind is spherically symetric and optically thin, it is then possible to estimate the velocity regime of the line formation using the deprojected emission function (Lépine & Moffat 1999). In Table 1 is listed in the third column the value $\langle v \rangle$, which is the velocity regime where the maximum emissivity of the line occurs, and in the fourth column the value Δv, which is the extension of the line formation region in velocity space for 4 different lines in the spectrum of WR3. Also are shown the same values for the He II λ4686 line of WR2 and WR152, two other WNE stars that we observed to compare with WR3.

Table 1: Line formation region

Star	Transition	$\langle v \rangle$ (km s^{-1})	Δv (km s^{-1})
WR3	N III λ4604	155-1500±10	60-900±5
	N V λ4620	145-1500±10	60-900±5
	He II λ4686	1520±5	900±5
	N V λ4945	145±5	60±5
WR2	He II λ4686	2340±5	750±5
WR152	He II λ4686	1240±5	610±5

The formation region of the He II λ4686 line of the three stars spans over a wide velocity range, going from moderate velocities to velocities near v_∞ (WR2: $v_\infty = 3100\,\mathrm{km\,s^{-1}}$, WR3: $v_\infty = 2500\,\mathrm{km\,s^{-1}}$ and WR152: $v_\infty = 2000\,\mathrm{km\,s^{-1}}$; Hamann et al. 1995). One can also see in Table 1 that the formation region of the N V λ4945 line in WR3 occurs at very low velocity. This allows us to probe radii near the base of the wind. Interestingly, both N III λ4604 and N V λ4620 present two components in the deprojected emission function, i.e. one at low and one at high velocity.

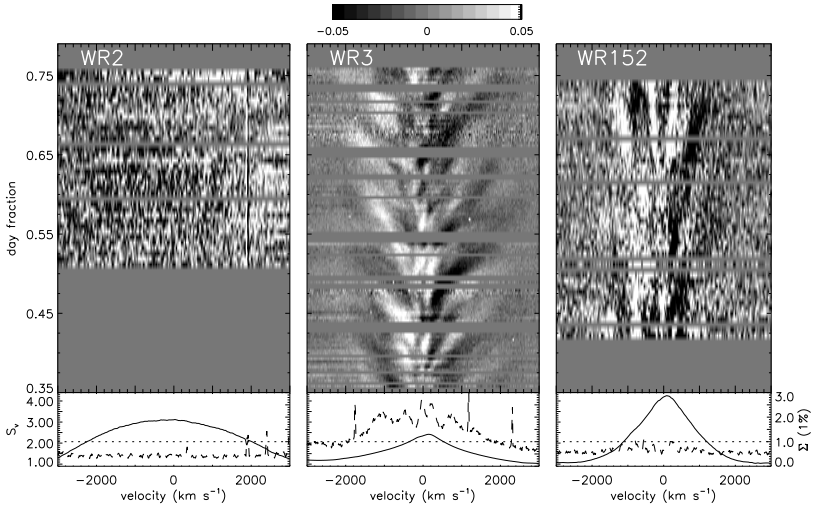

Figure 1: Spectral variability of the He II λ4686 line for WR2, WR3 and WR152. *Bottom panel*: Mean spectrum (solid line) and Σ spectrum (dashed line). Σ is proportional to the variability at each wavelength. The variability at a given wavelength is significant if Σ is higher than 1.0 (dotted line). *Upper panel*: Time-resolved plot of the residuals after subtracting the mean spectrum.

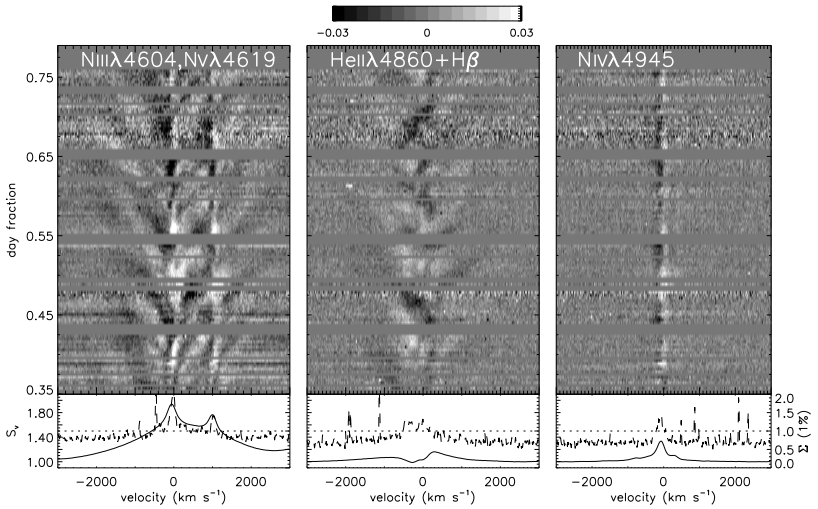

Figure 2: As in Fig. 1, but for N III λ4604 and N V λ4620 (left), He II λ4860 (middle) and N V λ4945 (right) in WR3.

3 Spectral Variability and the Velocity Law

Intense time-series of high-resolution spectra of the three WNE stars have been obtained at the Observatoire du mont Mégantic. Three nights were dedicated to WR2, eight to WR3 and six to WR152. Spectra with mean SNR $\sim$ 90 were obtained every 10 minutes. During an additional night at the William Hershel Telescope, spectra of WR3 with a mean SNR $\sim$ 120 were obtained every 5 minutes, allowing the analysis of weak-lines such as N V λ4945 line.

In Fig. 1 we present in the *upper panel* one example of the spectral variability observed during one night on the He II λ4686 line of the three stars WR2, WR3 and WR152. In the *lower panel* is plotted the Σ spectrum (Fullerton et al. 1996). If the value of Σ is higher than 1.0 at a given wavelength, this means that the spectrum is significantly variable at this wavelength at a confidence level of 99 %. For the three stars follow details.

3.1 WR2 (WN2)

Surprisingly, no variability at all was observed for WR2, even if the signal-to-noise ratio (SNR) was sufficiently high to allow a 2-3σ detection of a subpeak as small as 1% of the He II λ4686 line intensity, for a temporal resolution of 10 minutes. Moreover, the Σ spectrum never reaches a value higher than 1.0 all along the spectrum. Thus, no value of βR_* can be determined for this star.

3.2 WR3 (WN3ha)

While the spectrum of all the stars studied by Lépine & Moffat (1999) show slowly moving subpeaks that last for $\sim$ 10 hours, the spectrum of WR3, on the other hand, shows subpeaks that appear stochastically on the emission lines, move rapidly toward the edges of the line, and disappear within $\sim$3 hours. The curvature of the subpeak trajectories on the He II λ4686 line indicates that the acceleration of the wind at radii corresponding to its formation region is not constant. These subpeaks have an intensity of 1-1.5 % of the line intensity. In Fig. 2, we present the spectral variability of emission lines due to N III λ4604, N V λ4620, He II λ4686, He II λ4860 and N V λ4945. When comparing all these lines, we see they all are variable, that their subpeaks all lie between 1.0 and 1.5 % of the line intensity, and that the pattern of variability is comparable for lines sharing similar formation regions. Indeed, the trajectories of the subpeaks are similar on the He II λ4686 and He II λ4860+Hβ lines, but are not clearly associated with the the trajectories traced on the N V λ4945 line. Interestingly, the two N III λ4604 and N V λ4620 lines show a variability pattern that resembles a combination of the variability pattern of the He II λ4686 and the N V λ4945 lines.

To determine the velocity law of WR3, we first assume that the acceleration of clumps is not too far from a constant value. Then we can deduce a mean radial velocity ($v_{\rm m}$) and a mean radial acceleration ($a_{\rm m}$) of each clump with a linear regression of their trajectory. The relation $a_{\rm m}(v_{\rm m})$ is approximated by (Lépine & Moffat 1999) :

$$a_{\rm m}(v_{\rm m}) = \frac{\left[v_{\rm m} \ln(\frac{v_{\rm m}}{\mu v_\infty})\right]^2}{\mu \beta R_*}, \qquad (1)$$

where μ is the cosine of the angle of the clump trajectory with the line-of-sight, and βR_* is the parameter to be determined. In Fig. 3, each trajectory for a subpeak on the line He II λ4686 is represented by a point in the plot $a_{\rm m}(v_{\rm m})$. All these points cannot be fitted, because the change of μ from one trajectory to another implies different values of $a_{\rm m}(v_{\rm m})$, even with a single value of βR_* for all trajectories. However, βR_* can be estimated from the two curves of $a_{\rm m}$ with μ=-1 and μ=1 that englobe the bulk of the points. In Fig. 3 are plotted two different solutions of βR_* possible within the uncertainties of the measurements. As a result, βR_*=2.8-3.1 $R_\odot$ for WR3. Then, if R_*=2,5 $R_\odot$ (Hamann et al. 1995), β=1.1-1.2, a value significantly lower than what was determined for previously studied WR stars (Lépine & Moffat 1999). One can see that in Fig. 3, no point is present in the area near $a_{\rm m}$=0, defined by the curve $a_{\rm m}(v_{\rm m})$ and the dashed line. Then, at a velocity too high with an acceleration too low, no clump is present. This can be translated to a maximum radius where clumps are seen on the He II λ4686 line, leading to $R_{\rm max}$=3.5 $R_\odot$.

3.3 WR152 (WN3)

The motion of the subpeaks on the lines of WR152 is not as rapid as the motion of subpeaks on the lines of WR3 and lasts for $\sim$ 10 hours. However, from the $a_{\rm m}(v_{\rm m})$ curves, we deduce βR_*=5.0-7.0 $R_\odot$. If R$_*$=2.7 R$_\odot$ (Hamann et al. 1995), β=1.9-2.6. This is an intermediate case between WR3 and the stars of Lépine & Moffat (1999). No $R_{\rm max}$ could be deduced.

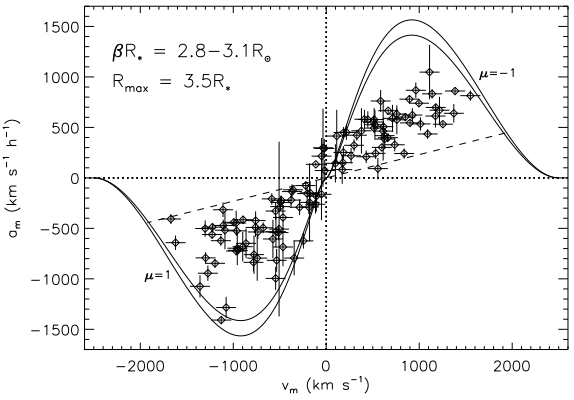

Figure 3: Comparison of $a_{\rm m}$ and $v_{\rm m}$ for all the clumps on He II λ4686 in WR3. In solid lines are plotted two solutions for βR_* = 2.8 and 3.1 $R_\odot$. The dashed line gives $R_{\rm max}$.

References

Fullerton, A.W., Gies, D.R., & Bolton, C.T. 1996, ApJS, 103, 475

Hamann, W.-R. et al. 1995, A&A, 299, 151

Lépine, S., & Moffat, A.F.J. 1999, ApJ, 514, 909

Marchenko, S.V. et al. 2004, MNRAS, 353, 153

Prinja: Since line profile variability is so widespread in WR stars and OB stars, it is very interesting when you come across a star that does *not* vary! Can you comment on what might be special in the case of WR2, where the lines are so steady and there is no evidence for moving sub-peaks on the emission lines?

Chene: Not that much. All I can say is, assuming that clumping produces line-profile variability of a level of 1 % of the line intensity, according to our signal to-noise ratio, we should have seen moving sub-peaks, if there were any. Maybe the lines observed in WR2 are formed in a highly optically thick region.

Hamann: Your results show that clumping is a universal phenomenon in WN stars of all sub-types, with the one exception you have shown, WR2, where you found no line-profile variability. I want to point out that WR2 has a very peculiar spectrum. Among all galactic WN, it is the only one which shows round-shaped emission-line profiles. (There is a similar counterpart in the LMC.) Such round-shaped profiles cannot be reproduced by the models at all. In Hamann et al. (2006,A&A 457) we have shown that a convolution with rotational broading gives a good fit to the observation, if $v_{\rm rot} \sin i = 1\,900\,{\rm km/s}$ is assumed. This demonstrates that something very strange is going on with WR2.

Ignace: In some cases, $\beta\, R_*$ is quite small. To what extent does the assumption of a β-law bias your implied values of R_*?

Chene: Maybe I did not make my point clear enough, but a small $\beta\, R_*$ does not imply a small R_*, but a small value of β. The value for R_* is taken from literature (e. g. Hamann 1995).

Hamann: I want to emphasize that the value of $\beta\, R_*$ that one obtains from the analysis of line-profile variability depends sensitively on the adopted radius of formation for the considered spectral line. This formation radius can only be inferred from adequate model atmospheres.